Revue de Métallurgie **110**, 341–348 (2013)
© EDP Sciences, 2013
DOI: 10.1051/metal/2013077
www.revue-metallurgie.org

Revue de Métallurgie

Numerical prediction of the effects of material properties on strain behavior during equal channel angular pressing

M. Ebrahimi[1], F. Djavanroodi[1,2], C. Gode[3] and K.M. Nikbin[2]

[1] *Department of Mechanical Engineering, Iran University of Science and Technology, Tehran, Iran*
e-mail: mebrahimi@iust.ac.ir
[2] *Department of Mechanical Engineering, Imperial College, London, SW7, UK*
[3] *School of Denizli Vocational Technology, Program of Machine, Pamukkale University, 20100 Denizli, Turkey*

Key words:
Equal channel angular pressing; finite element modeling; material properties; strain behavior

Abstract – Equal channel angular pressing is both a novel and an industrialized process among severe plastic deformation methods to fabricate ultra-fine-grained metals and alloys. Verification of a three-dimensional finite element model which compares various strength coefficients and strain-hardening exponents (virtual materials) defined for the plastic deformation behavior of materials was performed with experimental tests. The virtual process numerically analyzed the effects of the strain behavior and pressing force. The results show that strength coefficient enhancement leads to decreased effective strain value, heterogeneous strain distribution and higher pressing force, and an increment in the strain-hardening exponent results in lower pressing force. However, this parameter does not have an obvious effect on the effective strain magnitude and strain dispersal uniformity. Furthermore, the highest imposed effective strain, the best strain distribution homogeneity and the lowest required punch load were achieved for the deformed material with the lowest strength coefficient and highest strain-hardening exponent.

Received 16 April 2013
Accepted 22 October 2013

During the last decade, severe plastic deformation (SPD) methods have been widely developed by researchers in the materials science field because of the principal benefits and advantages of these techniques in military, airspace, and especially medical applications and industries. In other words, encouraging economic forecasts for ultra-fine-grain (UFG) materials have led to much attention being paid to the generation and development of SPD processes with mass-production scale-up capacities [1–6]. Among all the SPD techniques such as accumulative roll bonding (ARB) [7], high pressure torsion (HPT) [8], constrained groove pressing (CGP) [9], etc., equal channel angular pressing (ECAP) [1] has attracted the most attention because of its low cost and feasibility of set-up.

The ECAP process includes imposing large shear strain on the specimen by pushing it through a die that consists of two channels with the same cross-sectional shape meeting at an angle to each other (die channel angle, Φ) [1]. Since the cross-section of the two channels is the same, the ECAPed sample can be reinserted into the entrance channel and pushed through the die again. Repeated pressing through the die accumulates sufficient strain to obtain materials with UFG structures [1, 10].

Effective strain magnitude, strain distribution uniformity at the cross-section and in the whole of the deformed sample, and pressing force are affected by several factors such as die channel angle and outer corner angle [11,12], friction coefficient [11,13], processing routes [14,15], back pressure [16,17], billet diameter [18], strain rate sensitivity [14, 16], processing temperature [19], pass number [20,21], material response [22], kind of solution treatment [23], etc. Effective strain (ES) is defined as the total true strain minus the recoverable strain for the overall elements. In other words, it can be said that ES is related to the residual true strain after unloading the elastic part. Previous

https://doi.org/10.1051/metal/2013077 Published online by Cambridge University Press
Article published by EDP Sciences

studies [11,12] showed that the level of the imposed plastic strain was increased by using an acute die channel angle or adding a friction coefficient value. Also, a lower die channel angle or higher friction coefficient leads to completely filling the outer corner of the die. In addition, although lower effective strain magnitude was obtained for a larger die channel angle, a better strain distribution uniformity was attained. The research by Oruganti et al. [13] showed an ECAPed sample with higher shear strain and better distribution was achieved by applying high back pressure with low friction. The investigation of the effect of routes on strain behavior indicated that route B_C gives better strain dispersal homogeneity as compared with the other ones for a die channel angle of 90° [14,15]. The study by Kim [24] showed that the strain rate was decreased by the die channel and outer corner angles. Furthermore, the effect of the outer corner angle on the strain rate is much greater than that of the die channel angle due to the expanded main deformation zone and decreased deforming time.

There are several empirical equations to describe experimental stress – strain curves such as Hollomon (Eq. (1)), Ludwik (Eq. (2)), Swift (Eq. (3)) and Voce (Eq. (4)) relationships:

$$\sigma = K\varepsilon^n \quad (1)$$

$$\sigma = \sigma_0 + K\varepsilon^n \quad (2)$$

$$\sigma = K(\varepsilon + \varepsilon_0)^n \quad (3)$$

$$\sigma = B - (B - A)\exp(-n\varepsilon) \quad (4)$$

where σ and ε are the true stress and true strain, respectively, and the other parameters are constants. Previous studies indicated that the Hollomon equation is the best for annealed metals with a cubic lattice, and also gives a less accurate result for pre-worked materials. In this research, the Hollomon relationship was applied to define the plastic behavior of material by considering that annealed pure aluminum was utilized for the ECAP process. In addition, K and n are the strength coefficient and strain-hardening exponent, respectively. This equation can be linearized by taking logarithms on both sides, and then a linear regression line can be determined and the parameters (K and n) will be easily calculated [25].

Up to now, several numerical studies have investigated the influence of material properties on the strain behavior. Finite element modeling (FEM), which is the most suitable procedure to direct explorations similar to the real circumstances, removes the need for experimental complexities. The result of investigations on the ECAP process by Dumoulin et al. [26] showed that the strain-hardening exponent has the most significant effect on the strain uniformity. The influences of material properties on the strain behavior and required punch force were studied by Djavanroodi and Ebrahimi [27] during equal channel angular pressing with parallel channels. They showed that various magnitudes of strain-hardening exponents do not have much effect on the pressing force value, but an increase in the magnitude of the strength coefficient causes a higher magnitude of pressing force. The results of the study on aluminum alloys by Karpuz et al. [28] indicated that strain-hardening constants affect the formation of the corner gap angle due to variations in the material flow and plastic deformation homogeneity in the deformation zone of an ECAP die. The findings showed that any increase in these parameters results in an increase in the angle of the corner gap. Although several studies have been carried out on the effects of these two parameters (K and n) on the strain responses and required pressing load, there is a lack of information regarding material properties' influences on the strain behavior and required force value.

In this research, numerical investigations using representative virtual material properties were carried out on the effective strain magnitude, strain distribution uniformity and required pressing force after the first pass of the ECAP process at room temperature.

1 Finite element modeling

The commercial finite element code, ABAQUS/Explicit software, was utilized in order to investigate the effects of material properties on the strain behavior and required force magnitude during the ECAP process at an ambient temperature. The die and punch were assumed to be discretely

https://doi.org/10.1051/metal/2013077 Published online by Cambridge University Press

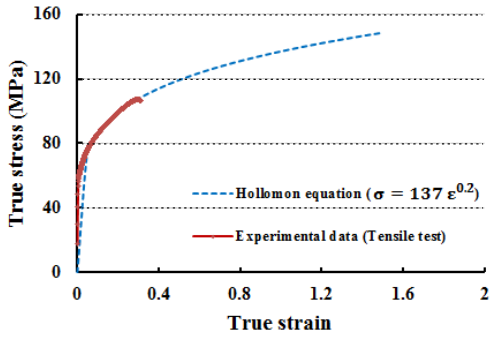


Fig. 1. True stress – strain curve of an annealed CP billet Al before the ECAP process obtained by a tensile test and curve fitting by the Hollomon model.

rigid, meaning that there is no deformation. The ECAP die characteristics are the same as in the experimental work. The constant punch speed was equal to 1 mm/s, similar to the experimental procedure. The magnitude of the friction coefficient was taken to be 0.1 [27]. This value was obtained by using the ring compression test for the ring 6:3:2 (outer diameter: inner diameter: height) and calibrated with the curves recommended by Male and Cockcroft [29]. Figure 1 displays the true stress – true strain curves of annealed commercial-purity (CP) aluminum obtained by a tensile test according to ASTM B557M (2010) and also, curve fitting with the Hollomon relationship, which was imported to the software. Furthermore, the stress – strain equation can be written as $\sigma = 137\,\varepsilon^{0.2}$. The length and diameter of the simulated sample were 50 mm and 19 mm, respectively. Adaptive meshing, mass scaling and automatic re-meshing were used and justified for all simulations to prevent failure of the mesh during large deformation and to reduce computation time. The mesh sensitivity diagram was attained, and then the optimum element size was found to be 0.7 mm. Also, the type of element was a three-dimensional hexahedral element (C3D8R). In addition, the number of elements for the CP billet aluminum was 19.750.

Verification of the numerical work was based on the required pressing force value to press CP billet aluminum after one pass of the ECAP process. After validation, various strength coefficients (K) and strain-hardening exponents (n) were numerically analyzed to investigate and compare the influences of material properties on the strain behavior, including effective strain magnitude and strain distribution uniformity, and required pressing load. Figure 2 displays the effective strain contour of the sample after one pass of the ECAP process.

2 Experimental procedure

A commercial-purity aluminum specimen (diameter of 19 mm and length of 50 mm) as a test material was prepared for this study. Before operation, the Al sample was annealed at 350 °C for 1 h and slowly cooled in the furnace. An ECAP die with a die channel angle of 90°, outer corner angle of 17° and channel diameter of 19 mm was designed and manufactured. The hydraulic press, die set-up and billet after one pass of the process are shown in Figure 3. All experimental work was done in the Research and Technology center at the Department of Mechanical Engineering of IUST. Molybdenum disulfide (MoS_2) was used as a lubricant to reduce frictional effects between the outer surface of the billet and the inner surface of the die channels. The ECAP process was performed at room temperature using a hydraulic press with a ram speed of 1 mm s^{-1}.

3 Results and discussion

3.1 Verification of FEM work

The ECAP die set-up in the experimental work was utilized to validate the simulation results. The magnitude of the required pressing force was measured in the laboratory and compared with the FEM results. After one pass, the pressing force magnitudes obtained by the experimental work and the simulation results are 51 KN and 47 KN, respectively. This represents about 8% discrepancy between the experimental and the numerical results, which for all practical purposes is acceptable.

3.2 Effect of material properties on the strain behavior

As is known, K and n are two important parameters for defining materials' plastic

https://doi.org/10.1051/metal/2013077 Published online by Cambridge University Press

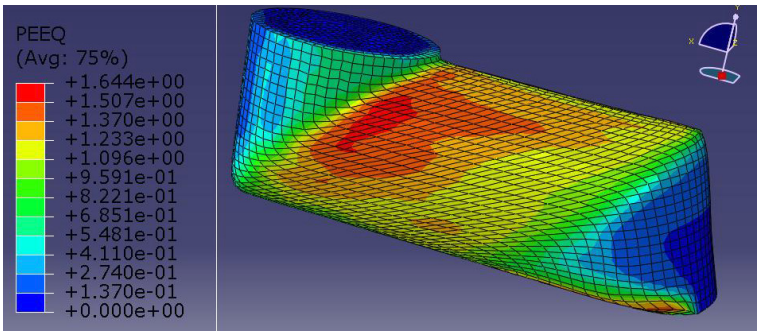


Fig. 2. Effective strain contour of billet Al after the first pass of the ECAP process.



Fig. 3. Hydraulic press, ECAP die set-up and CP billet Al after the first pass of pressing.

deformation behavior influencing the strain behavior of ECAPed samples, including the effective strain (ES) magnitude and strain distribution homogeneity. A numerical analysis was performed with materials of various strength coefficients (50, 100, 150, 150, 200, 250, 300 and 350 MPa) and strain-hardening exponents (0.20, 0.215, 0.230, 0.245, 0.260, 0.275, 0.290 and 0.305). These were numerically analyzed (56 different virtual materials), following which the influences of these two parameters on the strain behavior were investigated.

Figure 4 represents a contour plot of the imposed effective strain magnitude for 56 different K and n values during one pass of the ECAP process. It is apparent that a higher magnitude of effective strain was attained for the lower strength coefficient for the range of various strain-hardening exponents ($0.2 < n < 0.3$). Also, Figure 5 shows the effective strain magnitude for various strength coefficients, irrespective of the strain-hardening exponent. As can be seen, a low magnitude for the strength coefficient results in a high value for the effective strain magnitude. As an example, a 3% increase in the *ES* value can be obtained by applying material with K = 50 MPa instead of 350 MPa.

On the other hand, the effective strain magnitude for different strain-hardening exponents is represented in Figure 6, irrespective of the strength coefficient. It can be said that the magnitude of the strain-hardening exponent does not have any obvious effect on the *ES* value. As a result, the magnitude of K has more influence than n on the *ES* value during the ECAP process.

In general, two factors have been utilized to investigate strain distribution uniformity in order to demonstrate it quantitatively.

https://doi.org/10.1051/metal/2013077 Published online by Cambridge University Press

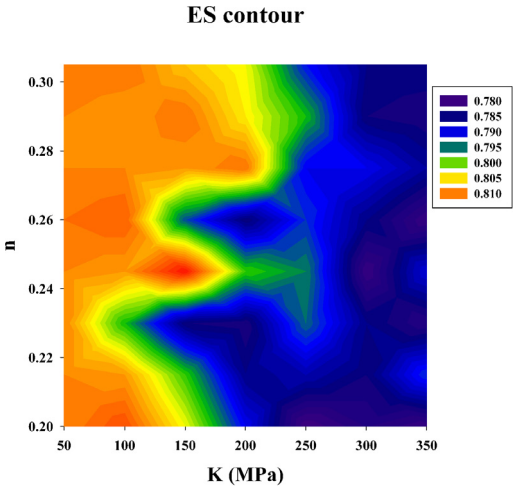


Fig. 4. Effects of various strength coefficients (*K*) and strain-hardening exponents (*n*) on the effective strain contour (*ES*) during one pass of the ECAP process.

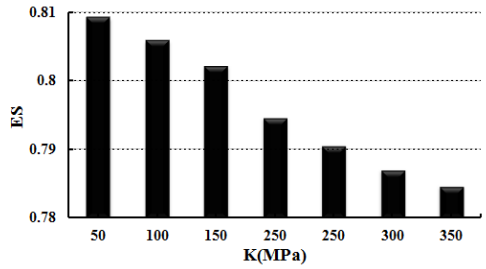


Fig. 5. Effective strain (*ES*) magnitude for different strength coefficients (*K*) after the first pass of the process, irrespective of the strain-hardening exponent.

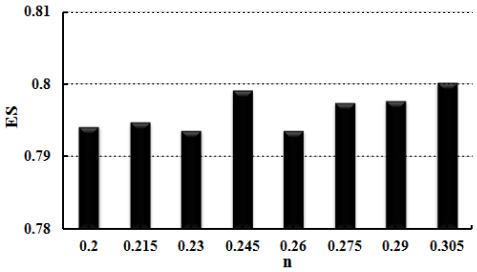


Fig. 6. Effective strain (*ES*) magnitude for different strain-hardening exponents (*n*) after the first pass of the process, irrespective of strength coefficients.

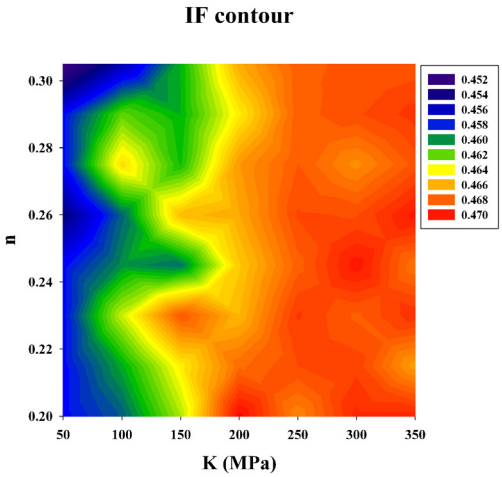


Fig. 7. Effects of various strength coefficients (*K*) and strain-hardening exponents (*n*) on the inhomogeneity factor (IF) contour during one pass of the ECAP process.

One is the inhomogeneity index (C_i), defined as [30]:

$$C_i = (\varepsilon_{max} - \varepsilon_{min})/\varepsilon_{ave} \qquad (5)$$

where ε_{max}, ε_{min} and ε_{ave} denote the maximum, minimum and average magnitude of effective plastic strain, respectively. A high value for the inhomogeneity index leads to heterogeneity for strain distribution. The other one is the inhomogeneity factor (IF), based on a statistical parameter which has been applied as follows [31]:

$$IF = \sqrt{\left(\sum_{i=1}^{n}(\varepsilon_i - \dot{\varepsilon})^2\right)}/(n-1) \qquad (6)$$

where ε_i, $\dot{\varepsilon}$ and n are the strain value at the ith element, mean strain value and number of elements, respectively. A lower magnitude for the IF leads to better uniformity for strain distribution. Therefore, the IF is a better factor to measure strain dispersal uniformity because it is based on the magnitude at all the nodes in the sample, where C_i is based on only two extreme magnitudes.

Figure 7 exhibits the inhomogeneity factor of strain distribution uniformity after 1 pass of the ECAP process using a contour plot. The graphical analysis shows that a deformed sample with better strain distribution homogeneity can be achieved for a lower strength coefficient when different strain-hardening exponents of 0.2 to 0.3 are examined. Furthermore, the effect of material properties (K and n) on the inhomogeneity factor

https://doi.org/10.1051/metal/2013077 Published online by Cambridge University Press

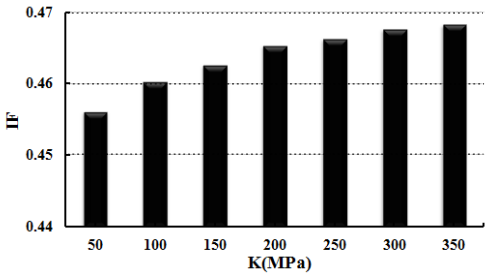


Fig. 8. Inhomogeneity factor (IF) values for various strength coefficients (*K*) after 1 pass of the ECAP process, irrespective of the strain-hardening exponent.

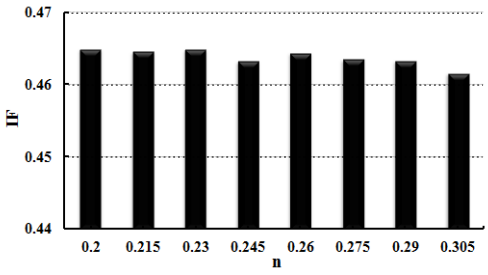


Fig. 9. Inhomogeneity factor (IF) values for various strain-hardening exponents (*n*) after 1 pass of the ECAP process, irrespective of the strength coefficient.

is investigated individually. Figure 8 shows IF values for various strength coefficients (K), irrespective of the strain-hardening exponent (n). As can be observed, strain distribution uniformity decreases by adding the strength coefficient. It means that a lower magnitude for k leads to producing material with better strain distribution homogeneity. For example, about 3% improvement in the uniformity of strain dispersal can be achieved by applying material with K = 50 MPa instead of 350 MPa.

On the other hand, various strain-hardening exponents (n) have a negligible effect on the IF value, irrespective of the strength coefficient (K); see Figure 9. As a result, K has more impression than n on the IF value during the ECAP process.

As a summary of this section, the magnitude of the strength coefficient has more influence than the strain-hardening exponent from the effective strain value and strain distribution uniformity points of view. Also, higher imposed effective strain with

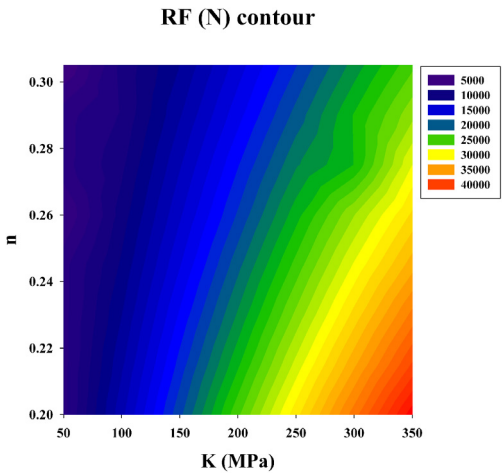


Fig. 10. Effects of various strength coefficients (*K*) and strain-hardening exponents (*n*) on the pressing force contour (RF) during one pass of the ECAP process.

better strain dispersal uniformity was attained for the material with a lower strength coefficient.

3.3 Effect of material properties on the pressing force

The influence of the strength coefficient and strain-hardening exponent on the required punch load is shown in Figure 10 as a contour plot form. The figure depicts that the lowest and highest required pressing force during the ECAP process were acquired for the samples with (lower K and higher n) and (higher K and lower n), respectively. Also, this finding can be shown using ultimate tensile strength (UTS). The UTS value can be obtained using the strength coefficient and strain-hardening exponent as follows:

$$UTS = K(n/e)^n \qquad (7)$$

where e is the base of the natural logarithm. According to the above relationship, the lowest RF value is related to the UTS = 26 MPa (K = 50 MPa and n = 0.305) and the highest RF magnitude is assigned to the UTS = 208 MPa (K = 350 MPa and n = 0.2), which is consistent with the above explanation.

The required force (RF) magnitude to press materials with various strength coefficients and strain-hardening exponents is also represented in Figures 11 and 12.

https://doi.org/10.1051/metal/2013077 Published online by Cambridge University Press

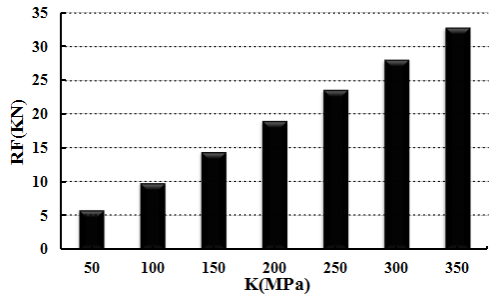


Fig. 11. Required pressing force values (RF) for materials with different strength coefficients (*K*), irrespective of the strain-hardening exponent.

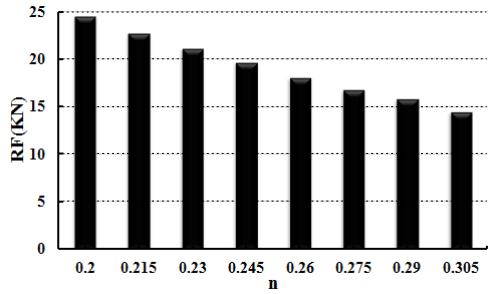


Fig. 12. Required pressing force values (RF) for materials with different strain-hardening exponents (*n*), irrespective of the strength coefficient.

As can be seen in Figure 11, an increasing strength coefficient leads to a higher required pressing force. For example, using K = 50 MPa instead of 350 MPa results in a 440% increase in the RF magnitude. On the other hand, it is noted from Figure 12 that an increment in the strain-hardening exponent results in a decrease in the pressing load. As an example, about 40% reduction can be obtained by using material with n = 0.2 instead of 0.305. On the whole, K has much more effect than n on the RF value during the ECAP process.

4 Conclusion

In this work, a detailed numerical analysis of the influences of material properties on the strain behavior and required force was performed using FEM. To validate the simulated results, an ECAP die with Φ = 90°, Ψ = 17° and channel diameter of 19 mm was designed and manufactured. The influence of various strength coefficients and strain-hardening exponents, defined for the plastic behavior of materials, was numerically simulated on the effective strain magnitude, strain distribution uniformity using an inhomogeneity factor and the required pressing force. Increasing the strength coefficient results in a lower effective strain magnitude, strain dispersal heterogeneity and higher punch load value. On the other hand, an increment in the strain-hardening exponent has a negligible effect on the *ES* and IF values, but leads to a lower RF magnitude. It clearly means that the K value has more influence than the n value on the *ES*, IF and even RF magnitude during the ECAP process. Furthermore, the highest imposed effective strain, the best strain distribution homogeneity and lowest required punch load were attained for the ECAPed processed material with the lowest strength coefficient and highest strain-hardening exponent.

References

[1] R.Z. Valiev, T.G. Langdon, *Prog. Mater. Sci.* **51** (2006) 881-981
[2] R. Song, D. Ponge, D. Raabe, J.G. Speer, D.K. Matlock, *Mater. Sci. Eng. A* **441** (2006) 1-17
[3] R. Srinivasan, P.K. Chaudhury, B. Cherukuri, Q. Han, D. Swenson, P. Gros, Continuous Severe Plastic Deformation Processing of Aluminum Alloys, Final Technical Report
[4] H.J. Rack, J.I. Qazi, *Mater. Sci. Eng. C* **26** (2006) 1269-1277
[5] A. Balakrishnan, B.C. Lee, T.N. Kim, B.B. Panigrahi, *Artif. Organs* **22** (2008) 58-64
[6] G. Serra, L. Morais, C.N. Elias, I.P. Semenova, R. Valiev, G. Salimgareeva, M. Pithon, R. Lacerda, *Mater. Sci. Eng. C* (2013)
[7] M. Shaarbaf, M.R. Toroghinejad, *Mater. Sci. Eng. A* **473** (2008) 28-33
[8] T. Hebesberger, H.P. Stüwe, A. Vorhauer, F. Wetscher, R. Pippan, *Acta Mater.* **53** (2005) 393-402
[9] A. Sajadi, M. Ebrahimi, F. Djavanroodi, *Mater. Sci. Eng. A* **552** (2012) 97-103
[10] Z. Jing, Z. Ke-shi, W. Hwai-Chung, Y. Mei-hua, *Trans. Nonferrous Met. Soc. China* **19** (2009) 1303-1311
[11] F. Djavanroodi, M. Ebrahimi, *Mater. Sci. Eng. A* **527** (2010) 1230-1235
[12] A.V. Nagasekhar, Y. Tick-Hon, S. Li, H.P. Seow, *Mater. Sci. Eng. A* **410-411** (2005) 269-272

https://doi.org/10.1051/metal/2013077 Published online by Cambridge University Press

[13] R.K. Oruganti, P.R. Subramanian, J.S. Marte, M.F. Gigliotti, S. Amancherla, *Mater. Sci. Eng. A* **406** (2005) 102-109

[14] N.E. Mahallawy, F.A. Shehata, M.A.E. Hameed, M.I.A.E. Aal, H.S. Kim, *Mater. Sci. Eng. A* **527** (2010) 1404-1410

[15] S. Bin-qing, C. Rong-shi, K. Wei, *Trans. Nonferrous Met. Soc. China* **21** (2011) 830-835

[16] V.V. Stolyarov, R. Lapovok, *J. Alloys Compd.* **378** (2004) 233-236

[17] Il-Heon Son, Jeong-Ho Lee, Yong-Taek Im, *J. Mater. Process. Technol.* **171** (2006) 480-487

[18] X. Zhang, L. Hua, Y. Liu, *Mater. Sci. Eng. A* **535** (2012) 153-163

[19] Z. Kai-feng, Y. Hong-hua, *Trans. Nonferrous Met. Soc. China* **19** (2009) s307-s311

[20] Z. Xiao-hua, L. Shou-jing, D. Zhi-ming, *Trans. Nonferrous Met. Soc. China* **18** (2008) 92-98

[21] F. Xiao-ming, A. Tao-tao, *Trans. Nonferrous Met. Soc. China* **19** (2009) 293-298

[22] S. Li, M.A.M. Bourke, I.J. Beyerlein, D.J. Alexander, B. Clausen, *Mater. Sci. Eng. A* **382** (2004) 217-236

[23] P. Venkatachalam, S.R. Kumar, B. Ravisankar, V.T. Paul, M. Vijayalakshmi, *Trans. Nonferrous Met. Soc. China* **20** (2010) 1822-1828

[24] H.S. Kim, M.H. Seo, S.I. Hong, *J. Mater. Process. Technol.* **130–131** (2002) 497-503

[25] Z. Gronostajski, *J. Mater. Process. Technol.* **106** (2000) 40-44

[26] S. Dumoulin, H.J. Roven, J.C. Werenskiold, H.S. Valberg, *Mater. Sci. Eng. A* **410–411** (2005) 248-251

[27] F. Djavanroodi, M. Ebrahimi, *Mater. Sci. Eng. A* **527** (2010) 7593-7599

[28] P. Karpuz, C. Simsir, C. Hakan Gür, *Mater. Sci. Eng. A* **503** (2009) 148-151

[29] A.T. Male, M.G. Cockcroft, *J. Inst. Met.* **93** (1964) 38-46

[30] H. Hong-jun, Z. Ding-fei, P. Fu-sheng, *Trans. Nonferrous Met. Soc. China* **20** (2010) 259-266

[31] V.P. Basavaraj, U. Chakkingal, T.S.P. Kumar, *J. Mater. Process. Technol.* **209** (2009) 89-95

https://doi.org/10.1051/metal/2013077 Published online by Cambridge University Press